Irreversible magnetization of pin-free type-II superconductors

Ernst Helmut Brandt
Max-Planck-Institut für Metallforschung, D-70506 Stuttgart, Germany
(Received 23 July 1999)

The magnetization of ideal type-II superconductors without vortex pinning is derived from first principles for superconductors with constant thickness. This magnetization is irreversible due to a macroscopic geometric barrier for flux penetration at the edges, which yields a sharply defined entry field H_{en}. Above some reversibility field $H_{rev}>H_{en}$ the magnetization becomes reversible and coincides with that of an ideal ellipsoid. [S0163-1829(99)04441-0]

It is commonly agreed that the irreversible magnetic behavior of type-II superconductors is due to pinning of the Abrikosov vortices at inhomogeneities in the material. However, similar hysteresis effects were also observed[1] in type-I superconductors, which do not contain flux lines, and in type-II superconductors with negligible pinning. In these two cases the magnetic irreversibility is caused by a geometric (specimen-shaped dependent) barrier that delays the penetration of magnetic flux but not its exit. In this respect the *macroscopic* geometric barrier behaves similar to the *microscopic* Bean-Livingston barrier[2] for straight vortices penetrating a parallel surface. In this paper I derive the static magnetization of pin-free type-II superconductors and its geometry-caused irreversibility *from first principles*, with no additional assumptions but given geometry. This universal solution should allow us to detect signatures of other barriers in experiments.

The geometric irreversibility is most pronounced for thin films of constant thickness in a perpendicular field. It is absent only when the superconductor is of exactly ellipsoidal shape or is tapered like a wedge with a sharp edge where flux penetration is facilitated. In ellipsoids the inward directed driving force exerted on the vortex ends by the surface screening currents is exactly compensated by the vortex line tension,[3] and thus the magnetization is reversible. In specimens with constant thickness (i.e., rectangular cross section) this line tension opposes the penetration of flux lines at the four corner lines, thus causing an edge barrier; but as soon as two penetrating vortex segments join at the equator they contract and are driven to the specimen center by the surface currents, see Fig. 1 below. As opposed to this, when the specimen profile is tapered and has a sharp edge, the driving force even in a very weak applied field exceeds the restoring force of the line tension such that there is no edge barrier. The resulting absence of hysteresis in wedge-shaped samples was nicely shown by Morozov *et al.*[4]

An elegant analytical theory of the field and current profiles in thin superconductor strips with an edge barrier has been presented by Zeldov *et al.*,[5] see also the extensions Ref. 6. With increasing applied field H_a, the magnetic flux does not penetrate until an entry field H_{en} is reached; at $H_a=H_{en}$ the flux immediately jumps to the center, from where it gradually fills the entire strip or disk. This behavior in increasing H_a is similar to that of thin films with artificially enhanced pinning near the edge,[6,7] but in decreasing H_a the behavior is different: In films with enhanced edge pinning (critical current density J_c^{edge}), the current density J at the edge immediately jumps from $+J_c^{edge}$ to $-J_c^{edge}$ when the ramp rate reverses its sign, while in pin-free films with geometric barrier the current density at the edge first stays constant or even increases and then gradually decreases and reaches zero at $H_a=0$. The entry field H_{en} was estimated for pin-free thin strips in Refs. 5 and 8, see also Ref. 9.

In this paper the geometry-caused magnetic irreversibility of ideal pin-free type-II superconductors is calculated for the two most important examples of circular disks (or cylinders)

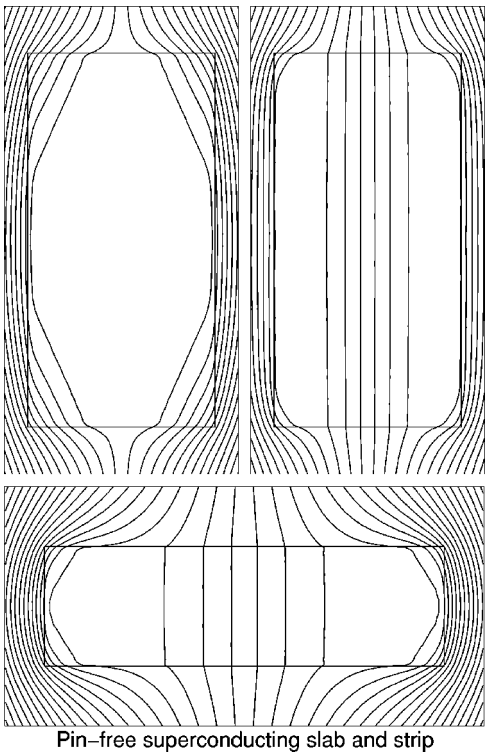

FIG. 1. The magnetic field lines of $\mathbf{B}(x,y)$ in slabs or strips with aspect ratio $b/a=2$ (top) and $b/a=0.3$ (bottom) in perpendicular magnetic field H_a. Top left: $H_a/H_{c1}=0.66$, in increasing field shortly below the entry field $H_{en}/H_{c1}=0.665$. Top right: $H_a/H_{c1}=0.5$, decreasing field. Bottom: $H_a/H_{c1}=0.34$ in increasing field just above $H_{en}/H_{c1}=0.32$. The field lines of cylinders look very similar. Note the straight field lines in the corners, corresponding to flux lines under tension.

and long strips (or slabs) with rectangular profile of arbitrary aspect ratio b/a. I present flux-density profiles and magnetization loops and give explicit expressions for the entry field H_{en} and for the reversibility field H_{rev} above which the magnetization curve is reversible. Finally, the modification of these results by volume pinning is briefly discussed.

First consider the known magnetization of ideal ellipsoids. If the superconductor is homogeneous and isotropic, the magnetization curves $M(H_a;N)$ are *reversible* and may be characterized by a demagnetizing factor N with $0 \leqslant N \leqslant 1$. If H_a is along one of the three principal axes of the ellipsoid, then N is a scalar. One has $N=0$ for long specimens in the parallel field, $N=1$ for thin films in the perpendicular field, and $N=1/3$ for spheres. If the magnetization curve in the parallel field is known, $M(H_a;0)=B/\mu_0 - H_a$, where B is the flux density inside the ellipsoid, then the homogeneous magnetization of the general ellipsoid, $M(H_a;N)$, follows from the implicit equation

$$H_i = H_a - N\,M(H_i;0). \tag{1}$$

Solving Eq. (1) for the effective internal field H_i, one obtains $M=M(H_a;N)=M(H_i;0)$. In particular, for the Meissner state ($B\equiv 0$) one finds $M(H_a;0)=-H_a$ and

$$M(H_a;N) = -\frac{H_a}{1-N} \quad \text{for} \quad |H_a| \leqslant (1-N)H_{c1}. \tag{2}$$

At the lower critical field H_{c1} one has $H_i=H_{c1}$, $H_a=H'_{c1}=(1-N)H_{c1}$, $B=0$, and $M=-H_{c1}$. Near the upper critical field H_{c2} one has an approximately linear $M(H_a;0)=\gamma(H_a-H_{c2})<0$ with $\gamma>0$, yielding

$$M(H_a;N) = \frac{\gamma}{1+\gamma N}(H_a - H_{c2}) \qquad \text{for} \quad H_a \approx H_{c2}. \tag{3}$$

Thus, if the slope $\gamma \ll 1$ is small (and in general, if $|M/H_a| \ll 1$ is small), demagnetization effects may be disregarded and one has $M(H_a;N)\approx M(H_a;0)$.

The ideal magnetization curve of type-II superconductors with $N=0$, $M(H_a;0)$ or $B(H_a;0)/\mu_0 = H_a + M(H_a;0)$, may be calculated from Ginzburg-Landau (GL) theory,[10] but any other model curve may be used provided $M(H_a;0) = -M(-H_a;0)$ has a vertical slope at $H_a=H_{c1}$ and decreases monotonically in size for $H_a > H_{c1}$. For simplicity in this paper I shall assume $H_{c1} \ll H_{c2}$ (i.e., large GL parameter $\kappa \gg 1$) and $H_a \ll H_{c2}$. To illustrate the essential features I may thus use $M(H_a;0)=-H_a$ for $|H_a| \leqslant H_{c1}$ and the good approximation

$$M(H_a;0) = (H_a/|H_a|)(|H_a|^3 - H_{c1}^3)^{1/3} - H_a \tag{4}$$

for $|H_a| > H_{c1}$, see the curve labeled ∞ in Fig. 3 below.

In nonellipsoidal superconductors the induction $\mathbf{B}(\mathbf{r})$ in general is not homogeneous, and so the concept of a demagnetizing factor does not work. However, when the magnetic moment $\mathbf{m} = \frac{1}{2}\int \mathbf{r}\times\mathbf{J}(\mathbf{r})d^3r$ is directed along H_a, one may define an *effective demagnetizing factor N*, which in the Meissner state ($B\equiv 0$) yields the same slope $M/H_a = -1/(1-N)$, Eq. (2), as an ellipsoid with the same volume V. Here the definition $M=m/V$ with $m=\mathbf{m}H_a/H_a$ is used. For long strips and circular disks or cylinders with cross section $2a\times 2b$ in a perpendicular or axial magnetic field along the thickness $2b$, approximate expressions for the slopes $M/H_a = m/(VH_a)$ are given in Refs. 11 and 12. Using this and defining $q \equiv (|M/H_a|-1)(b/a)$, one obtains the effective N for any aspect ratio b/a in the form

$$N = 1 - 1/(1+qa/b),$$

$$q_{\text{strip}} = \frac{\pi}{4} + 0.64\tanh\left[0.64\frac{b}{a}\ln\left(1.7+1.2\frac{a}{b}\right)\right],$$

$$q_{\text{disk}} = \frac{4}{3\pi} + \frac{2}{3\pi}\tanh\left[1.27\frac{b}{a}\ln\left(1+\frac{a}{b}\right)\right]. \tag{5}$$

In the limits $b \ll a$ and $b \gg a$, formulas (5) are exact, and for general b/a the relative error is $<1\%$. For $a=b$ (square cross section) they yield for the strip $N=0.538$ (while $N=1/2$ for a circular cylinder in the perpendicular field) and for the short cylinder $N=0.365$ (while $N=1/3$ for the sphere).

Now we consider the full, irreversible magnetization curves $M(H_a)$ of pin-free strips and cylinders with cross section $2a\times 2b$. Appropriate continuum equations and algorithms (which apply also to pinning) have been proposed recently by Labusch and Doyle[13] and by the author,[14] based on the Maxwell equations and on constitutive laws that describe flux flow and pinning [or thermal depinning expressed, e.g., by an electric field $\mathbf{E}(\mathbf{J},\mathbf{B})$] and the equilibrium magnetization in absence of pinning, $M(H_a;0)$. Here I shall use the method[14] and the model $M(H_a;0)$, Eq. (4). The pin-free flux dynamics will be described as viscous motion by $\mathbf{E}=\rho_{\text{FF}}(B)\mathbf{J}$ with flux-flow resistivity $\rho_{\text{FF}}\propto B$, but our quasistatic results should be independent of the choice of ρ_{FF}. In both methods the $M(H_a;0)$ law enters the driving force density on the vortices, $\mathbf{J_H}\times\mathbf{B}$ with definition $\mathbf{J_H}=\nabla\times\mathbf{H}$, where $\mathbf{H}(\mathbf{B})$ is obtained by inverting the relation $\mathbf{B}(\mathbf{H})=\mathbf{H}+\mathbf{M}(\mathbf{H};0)$.

While the method in Ref. 13 considers a magnetic charge density on the specimen surface which causes an effective field $\mathbf{H}_i(\mathbf{r})$ inside the superconductor, our method[14] couples the arbitrarily shaped superconductor to the external field $\mathbf{B}(\mathbf{r},t)$ via surface screening currents: In a first step the vector potential $\mathbf{A}(\mathbf{r},t)$ is calculated for given current density $\mathbf{J}$; then this relation (a matrix) is inverted to obtain $\mathbf{J}$ for given $\mathbf{A}$ and given $\mathbf{H}_a$; next the induction law is used to obtain the electric field [in our symmetric geometry one has $\mathbf{E}(\mathbf{J},\mathbf{B}) = -\partial\mathbf{A}/\partial t$], and finally the constitutive law $\mathbf{E}=\mathbf{E}(\mathbf{J},\mathbf{B})$ is used to eliminate $\mathbf{A}$ and $\mathbf{E}$ and obtain one single integral equation for $\mathbf{J}(\mathbf{r},t)$ as a function of $\mathbf{H}_a(t)$, without having to compute $\mathbf{B}(\mathbf{r},t)$ outside the specimen. This method, in general, is fast and elegant; but so far the algorithm is restricted to aspect ratios $0.03 \leqslant b/a \leqslant 30$, and to a number of grid points not exceeding 1000 (on a personal computer). Improved accuracy is expected by combining methods used in Ref. 13 (working best for small b/a) and Ref. 14.

The penetration and exit of flux computed by the method in Ref. 14 is illustrated in Figs. 1 and 2 for isotropic strips and disks without volume pinning, using a flux-flow resistivity $\rho_{\text{FF}}=\rho B(\mathbf{r})$ with $\rho=140$ (strip) or $\rho=70$ (disk) in units where $H_{c1}=a=\mu_0=|dH_a/dt|=1$. The profiles of the induction $B_y(r,y)$ taken along the midplane $y=0$ of the thick disk in Fig. 2 have a pronounced minimum near the edge r

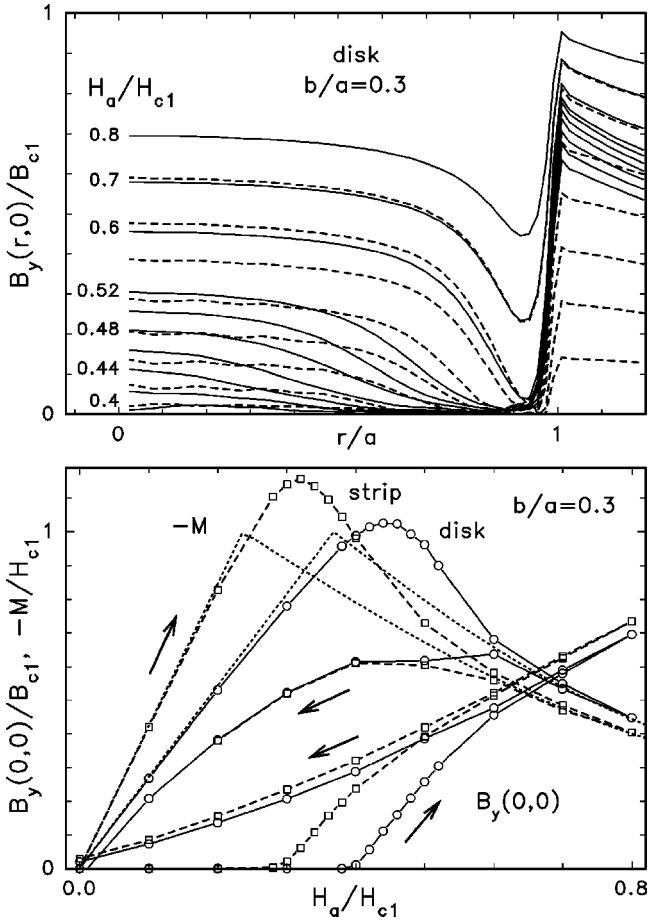

FIG. 2. Top: Profiles of the axial magnetic induction $B_y(r,y)$ in the midplane $y=0$ of a pin-free superconductor disk with aspect ratio $b/a=0.3$ in increasing field (solid lines) and then decreasing field (dashed lines), plotted at $H_a/H_{c1}=0.4$, 0.42, . . . , 0.5, 0.52, 0.6, 0.7, 0.8, 0.7, 0.6, . . . , 0.1, 0. $B_{c1}=\mu_0 H_{c1}$. Bottom: The induction $B_y(0,0)$ in the center of the same disk (solid line) and of a strip (dashed line), both with $b/a=0.3$. The symbols mark the field values at which the profiles are taken. Also shown is the magnetization loop for the same disk and strip and the corresponding reversible magnetization (dotted lines), see also Fig. 3.

$=a$, precisely in the region where strong screening currents flow. Away from the edges, the current density $\mathbf{J}=\nabla\times\mathbf{B}/\mu_0$ is nearly zero; note the parallel field lines in Fig. 1. The quantity $\mathbf{J_H}=\nabla\times\mathbf{H(B)}$ that enters the Lorentz force density $\mathbf{J_H}\times\mathbf{B}$, is even exactly zero since we assume absence of pinning. Our finite flux-flow parameter ρ and finite ramp rate $dH_a/dt=\pm 1$ mean a dragging force which, similar to pinning, causes a weak hysteresis and a small remanent flux at $H_a=0$; this artifact is reduced by choosing larger resistivity or slower ramping.

The induction $B_y(0,0)$ in the specimen center in Fig. 2 performs a hysteresis loop very similar to the magnetization loops $M(H_a)$ shown in Figs. 2 and 3. Both loops are symmetric, e.g., $M(-H_a)=-M(H_a)$. The maximum of $M(H_a)$ defines a field of first flux entry $H_{\rm en}$, which closely coincides with the field $H'_{\rm en}$ at which $B_y(0,0)$ starts to appear. The computed entry fields are well fitted by

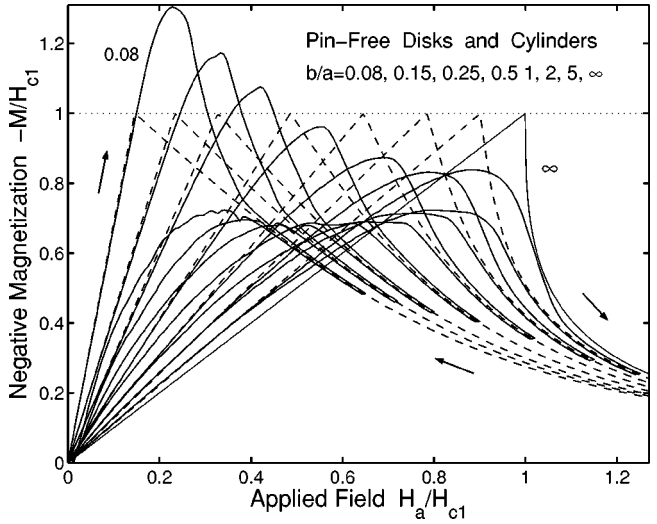

FIG. 3. Irreversible magnetization curves $-M(H_a)$ of pin-free circular disks and cylinders with aspect ratios $b/a=0.08$, 0.15, 0.25, 0.5, 1, 2, 5, and ∞ in axial field (solid lines). In these type-II superconductors the irreversibility is due to a purely geometric edge barrier for flux penetration. The dashed curves are the reversible magnetization curves of the corresponding ellipsoid defined by Eqs. (1), (4), and (5).

$$H_{\rm en}^{\rm strip}/H_{c1}=\tanh\sqrt{0.36b/a},$$

$$H_{\rm en}^{\rm disk}/H_{c1}=\tanh\sqrt{0.67b/a}. \qquad (6)$$

These formulas are good approximations for all aspect ratios $0<b/a<\infty$, see also the estimates of $H_{\rm en}\approx\sqrt{b/a}$ for thin strips in Refs. 5 and 8.

The virgin curve of the irreversible $M(H_a)$ of strips and disks at small H_a coincides with the ideal Meissner straight line $M=-H_a/(1-N)$ of the corresponding ellipsoid, Eqs.

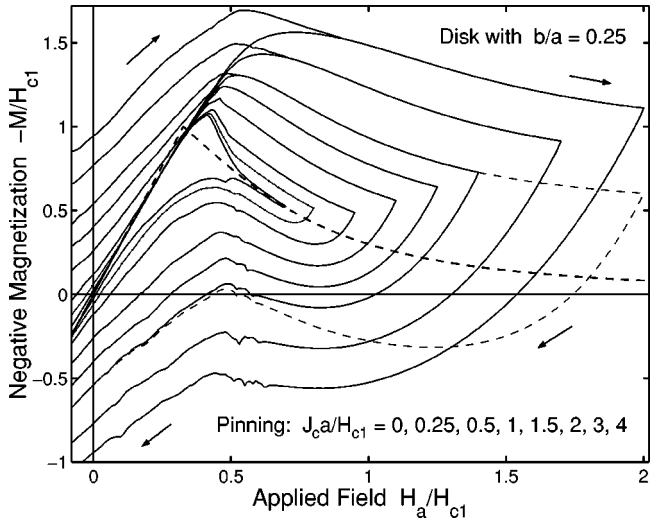

FIG. 4. Magnetization curves of a thick disk with aspect ratio $b/a=0.25$ for various degrees of volume pinning, $J_c=0$, 0.25, 0.5, 1, 1.5, 2, 3, 4 in units H_{c1}/a, and for various sweep amplitudes. The inner loop belongs to the pin-free disk ($J_c=0$), the outer loop to strongest pinning. Also shown is the reversible magnetization curve of the corresponding ellipsoid (dashed curve). All loops are symmetric, $M(-H_a)=-M(H_a)$.

(2) and (5). When the increasing H_a approaches H_{en}, flux starts to penetrate into the corners in the form of stretched flux lines (Fig. 1) and thus $|M(H_a)|$ falls below the Meissner line. At $H_a = H_{en}$ flux penetrates and jumps to the center, and $|M(H_a)|$ starts to decrease. In decreasing H_a, this barrier is absent. As can be seen in Fig. 3, above some field H_{rev}, the magnetization curve $M(H_a)$ becomes reversible and exactly coincides with the curve of the ellipsoid defined by Eqs. (1), (4), and (5) (in the quasistatic limit with $\rho^{-1} dH_a/dt \to 0$). The irreversibility field H_{rev} is difficult to compute since, in our present algorithm, it slightly depends on the choices of the flux-flow parameter ρ (or ramp rate) and of the numerical grid, and also on the model for $M(H_a;0)$. In the interval $0.08 \leqslant b/a \leqslant 5$ we find with relative error of 3%,

$$H_{rev}^{strip}/H_{c1} = 0.65 + 0.12 \ln(b/a),$$

$$H_{rev}^{disk}/H_{c1} = 0.75 + 0.15 \ln(b/a). \quad (7)$$

This fit obviously does not apply to $b/a \ll 1$ (since H_{rev} should exceed $H_{en} > 0$) nor to $b/a \gg 1$ (where H_{rev} should be close to H_{c1}). The limiting value of H_{rev} for thin films with $b \ll a$ is thus not known at present.

Remarkably, the irreversible magnetization curves $M(H_a)$ of pin-free strips and disks fall on top of each other if the strip is chosen twice as thick as the disk, $(b/a)_{strip} \approx 2(b/a)_{disk}$. This striking coincidence holds for all aspect ratios $0 < b/a < \infty$ and can be seen from each of Eqs. (5)–(7): The effective N [or virgin slope $1/(1-N)$], the entry field H_{en}, and the reversibility field H_{rev} are nearly equal for strips and disks with half thickness, or for slabs and cylinders with half length.

Another interesting feature of the pin-free magnetization loops is that the maximum of $|M(H_a)|$ exceeds the maximum of the reversible curve (equal to H_{c1}) when $b/a \leqslant 0.8$ for strips and $b/a \leqslant 0.4$ for disks, but at larger b/a it falls below H_{c1}. The maximum magnetization may be estimated from the slope of the virgin curve $1/(1-N)$, Eq. (5), and from the field of first flux entry, Eq. (6).

Finally, Fig. 4 shows how the irreversible magnetization loop is modified when volume pinning of the flux lines is switched on. Increasing critical current density J_c (in natural units H_{c1}/a) inflates the loops nearly symmetrically about the pin-free loop or (above H_{rev}) about the reversible curve, and the maximum of $|M(H_a)|$ shifts to higher fields. Above H_{rev} the width of the loop is nearly proportional to J_c, as expected from previous theories[11,12] that assumed $H_{c1} = 0$, but at small fields the influence of finite H_{c1} is clearly seen up to rather strong pinning.

In conclusion, Eqs. (5)–(7) and Figs. 1–3, derived from first principles with no assumptions but the geometry and finite H_{c1}, should be used to interpret experiments on superconductors with no or very weak vortex pinning. A detailed account of pinning and vortex dynamics will be published.

[1] J. Provost, E. Paumier, and A. Fortini, J. Phys. F **4**, 439 (1974); A. Fortini, A. Haire, and E. Paumier, Phys. Rev. B **21**, 5065 (1980).

[2] C. P. Bean and J. D. Livingston, Phys. Rev. Lett. **12**, 14 (1964); L. Burlachkov, Phys. Rev. B **47**, 8056 (1993).

[3] M. V. Indenbom, H. Kronmüller, T. W. Li, P. H. Kes, and A. A. Menovsky, Physica C **222**, 203 (1994); M. V. Indenbom and E. H. Brandt, Phys. Rev. Lett. **73**, 1731 (1994); E. H. Brandt, Rep. Prog. Phys. **58**, 1465 (1995).

[4] N. Morozov *et al.*, Physica C **291**, 113 (1997).

[5] E. Zeldov, A. I. Larkin, V. B. Geshkenbein, M. Konczykowski, D. Majer, B. Khaykovich, V. M. Vinokur, and H. Strikhman, Phys. Rev. Lett. **73**, 1428 (1994).

[6] E. Zeldov *et al.*, Physica C **235-240**, 2761 (1994); B. Khaykovich *et al.*, *ibid.* **235-240**, 2757 (1994); N. Morozov *et al.*, Phys. Rev. Lett. **76**, 138 (1996).

[7] Th. Schuster, M. V. Indenbom, H. Kuhn, E. H. Brandt, and M. Konczykowski, Phys. Rev. Lett. **73**, 1424 (1994).

[8] M. Benkraouda and J. R. Clem, Phys. Rev. B **53**, 5716 (1996); **58**, 15 103 (1998).

[9] I. L. Maksimov and A. A. Elistratov, Pis'ma Zh. Eksp. Teor. Fiz. **61**, 204 (1995) [JETP Lett. **61**, 208 (1995)]; A. V. Kuznetsov, D. V. Eremenko, and V. N. Trofimov, Phys. Rev. B **56**, 9064 (1997); **57**, 5412 (1998).

[10] E. H. Brandt, Phys. Rev. Lett. **78**, 2208 (1997).

[11] E. H. Brandt, Phys. Rev. B **54**, 4246 (1996).

[12] E. H. Brandt, Phys. Rev. B **58**, 6506 (1998); **58**, 6523 (1998).

[13] R. Labusch and T. B. Doyle, Physica C **290**, 143 (1997); T. B. Doyle, R. Labusch, and R. A. Doyle, *ibid.* **290**, 148 (1997).

[14] E. H. Brandt, Phys. Rev. B **59**, 3369 (1999).